

Article

Spectroscopic Behavior of Some A₃B Type Tetrapyrrolic Complexes in Several Organic Solvents and Micellar Media

Rica Boscencu ¹, Mihaela Ilie ^{1,*} and Radu Socoteanu ²

¹ Faculty of Pharmacy, “Carol Davila” University of Medicine and Pharmacy, 6 Traian Vuia Street, Bucharest 020956, Romania; E-Mail: rboscencu@yahoo.com

² “Ilie Murgulescu” Institute of Physical Chemistry, Romanian Academy, 202 Splaiul Independenței, Bucharest 060021, Romania; E-Mail: psradu@yahoo.com

* Author to whom correspondence should be addressed; E-Mail: m16ilie@yahoo.com;
Tel.: +4-021-3111152; Fax: +4-021-3111152.

Received: 20 June 2011; in revised form: 19 August 2011 / Accepted: 26 August 2011 /

Published: 30 August 2011

Abstract: The paper presents spectral studies of some unsymmetrical A₃B tetrapyrrolic, porphyrin-type complexes with Cu(II) and Zn(II) in different solvents and micellar media aimed at estimating their properties in connection with the living cell. The results indicate that the position of the absorption and emission peaks is mostly influenced by the central metal ion and less by the environmental polarity or the peripheric substituents of the porphyrinic core. The comparison between the overall absorption and emission spectra of the compounds in methanol or cyclohexane vs. direct and reverse Triton X micellar systems, respectively, suggests for all compounds the localization at the interface between the polyethylene oxide chains and the tert-octyl-phenyl etheric residue of the Triton X-100 molecules. These findings could be important when testing the compounds embedded in liposomes or other delivery systems to the targeted cell.

Keywords: unsymmetrical mesoporphyrinic complexes; micelles; solvatochromy; spectroscopy

1. Introduction

Spectroscopic characterization of porphyrins in different media is an important step in assessing their application in the biomedical field, as the matrix in which they are supposed to act is a complex one, involving both hydrophilic and lipophilic characteristics [1–7].

The amphiphilic character of the porphyrins, given by the hydrophobic and hydrophilic groups placed in various proportions and positions of the substituted structure, generates an intramolecular axis of polarity. This specific structure is responsible for the biological properties of porphyrins related to the cell membranes penetration and/or cellular target binding. When used in therapy (e.g., photodynamic therapy—PDT) or as markers (molecular probes in photodynamic diagnosis—PDD), their spectral properties are important characteristics that often define their efficiency as photosensitizers [8,9]. Because the lifetime of oxygen singlet ($^1\Delta_g$) in organic solvents or micelles is higher than in water, the singlet-oxygen-mediated photodamage will increase when the porphyrins are located in hydrophobic regions [10]. Also, the incorporation of porphyrins in micelles dramatically influences the aggregation characteristics and location of these molecules within the cells [11]. These are the main reasons to study the particular case of the A_3B unsymmetrically *meso*-substituted metalloporphyrins as amphiphilic structures in different polarity media and incorporated in nanostructures such as micelles [12–14].

Solvatochromy studies can also provide valuable information to identify the potential molecular targets within the cell [10], to predict the cellular intake and subsequent porphyrin metabolism [15] and to obtain optimum conditions for the photosensitization, as spectral properties are often dramatically changed by the microenvironment [16,17].

The non-ionic surfactants exhibit an extended polar part, with variable dimensions given by the number of oxyethylene units, which is highly influenced by hydration. Among this kind of surfactants, *tert*-octylphenoxypolyethoxyethanol (Triton X-100) has a polyoxyethylene chain consisting of 9.5 ethylene oxide units on average, thus being a medium-chain length surfactant [18]. Literature data indicate a general good understanding of the rules governing self-assembly in direct (DM) and reverse micelles (RM) built with this surfactant [19,20]. Therefore, we chose to work with two well characterized TX-100 micelle systems, having well-defined dimensions, aggregation numbers and core polarities (Figure 1). Polyethylene glycol (PEG) has been widely used in pharmaceutical preparations [21]. The similarity of PEG chemical structure allowed us to compare the spectral changes observed for the porphyrins embedded in DM and RM and to suggest the possible localization of the compounds tested within the micelles.

The study presents a few of such spectral properties for some unsymmetrical porphyrinic complexes which have been previously synthesized [22–24], and are presented in Figure 2: 5-[(3,4-methylenedioxy)phenyl]-10,15,20-*tris*-(4-carboxymethylphenyl)-21,23-Zn(II)-porphine (Zn(II)TRMOPP), 5-[(3,4-methylenedioxy)phenyl]-10,15,20-*tris*-(4-carboxymethylphenyl)-21,23-Cu(II)-porphine (Cu(II)TRMOPP), 5-(4-hydroxyphenyl)-10,15,20-*tris*-(4-carboxymethylphenyl)-21,23-Zn(II)-porphine (Zn(II)TCMPOHp), 5-(4-hydroxyphenyl)-10,15,20-*tris*-(4-carboxymethylphenyl)-21,23-Cu(II)-porphine (Cu(II)TCMPOHp), 5-(*x*-hydroxyphenyl)-10,15,20-*tris*-phenyl-21,23-Cu(II)-porphine (Cu(II)TPPOH_{*x*}), 5-(*x*-hydroxyphenyl)-10,15,20-*tris*-phenyl-21,23-Zn(II)-porphine (Zn(II)TPPOH_{*x*}) (*x* = 2, 3, 4).

Figure 1. General scheme of the porphyrinoid systems studied.

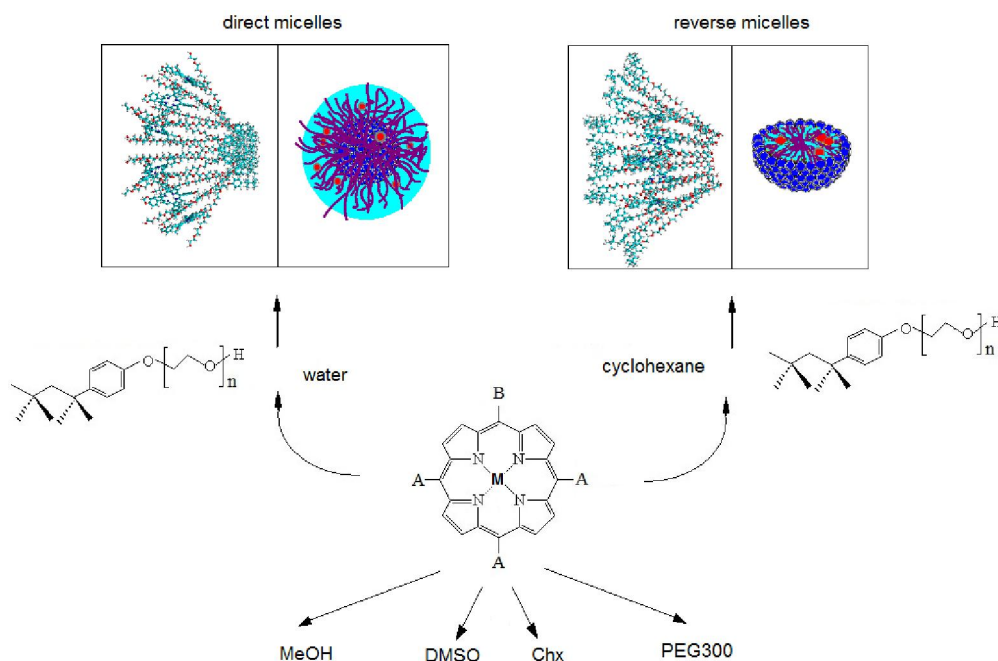
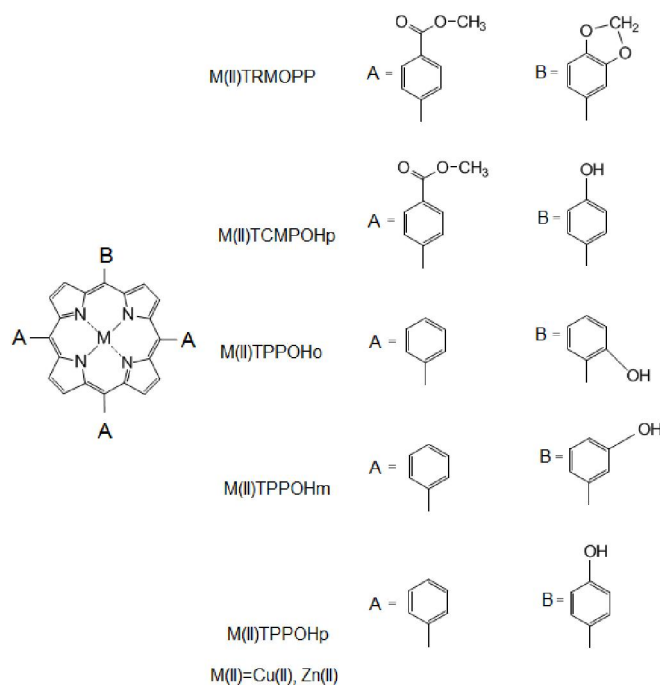


Figure 2. General structures of the unsymmetrical mesoporphyrinic complexes used in this study.



The spectral characteristics defined as follows could predict the spectral characteristics of protein-bound mesoporphyrinic systems and also the properties of the studied compounds in pharmaceutical formulation.

2. Results and Discussion

2.1. UV-Vis Spectroscopy

Porphyrinic complexes display in their molecular absorption spectra, one Soret (B) band as a result of $a_{1u}(\pi) \rightarrow e_g(\pi^*)$ transition, generally situated in the spectral range 400–440 nm, and one or two Q bands between 500–650 nm, corresponding to the $a_{2u}(\pi) \rightarrow e_g(\pi^*)$ transition [25,26].

The unsymmetrical mesoporphyrinic complexes used in this study revealed a strong Soret band with maximum in the range 410–430 nm accompanied by Q bands situated in the range 540–600 nm (Figure 3, Tables 1, 2). Results are consistent with those obtained on similar compounds [27].

Figure 3. Absorption spectra of 2.5×10^{-6} M Cu(II)TPPOH_m in different solvents and micellar solutions: (a) Soret band; and (b) Q band.

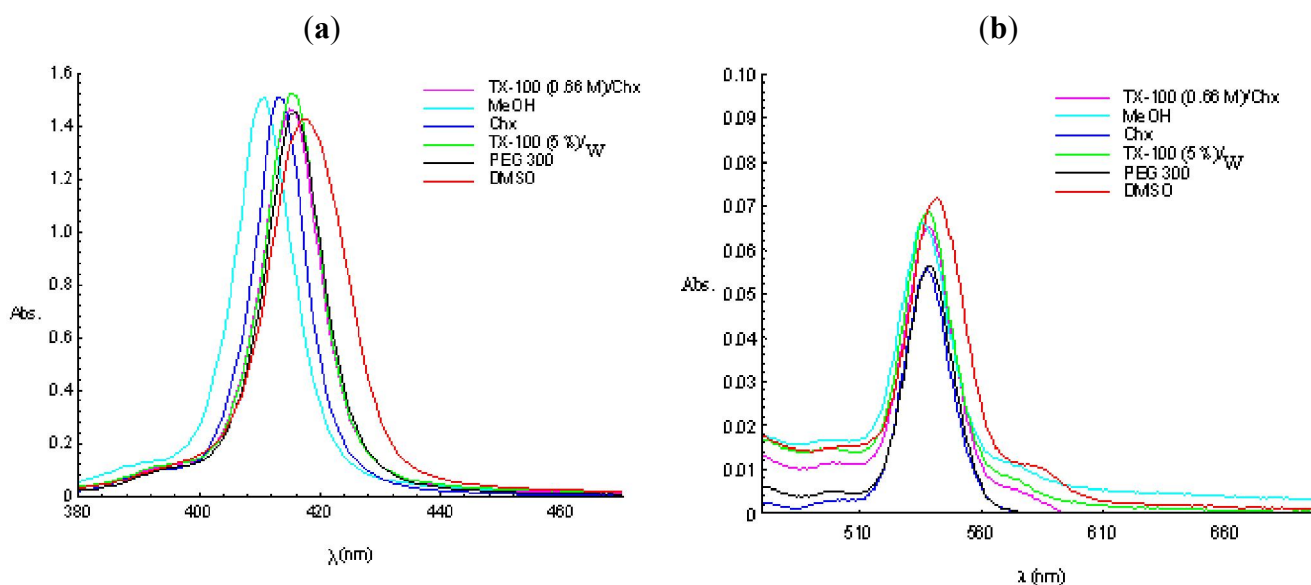


Table 1. Wavelengths maxima (λ_{\max}) and molar extinction coefficient values ($\lg \epsilon$) for the zinc porphyrinic complexes in different solvents and micellar media ($c = 2.5 \times 10^{-6}$ M).

Solvent	λ_{\max} (nm) [$\lg \epsilon$ ($L \text{ mol}^{-1} \text{ cm}^{-1}$)]		
	Soret B (0,0)	Q (1,0)	Q (0,0)
<i>5-(2-hydroxyphenyl)-10,15,20-tris-phenyl-21,23-Zn(II)-porphine</i>			
MeOH	421 [5.726]	556 [4.342]	595 [4.033]
DMSO	428 [5.695]	560 [4.326]	560 [4.121]
Chx	425 [5.570]	557 [4.191]	597 [3.741]
PEG300	426 [5.659]	558 [4.310]	597 [4.000]
TX/water	427 [5.674]	559 [4.357]	598 [4.342]
TX/Chx	427 [5.674]	559 [4.356]	598 [4.334]
<i>5-(3-hydroxyphenyl)-10,15,20-tris-phenyl-21,23-Zn(II)-porphine</i>			
MeOH	421 [5.867]	556 [4.394]	595 [3.982]
DMSO	428 [5.867]	559 [4.408]	600 [4.146]
Chx	425 [5.778]	557 [4.254]	596 [3.702]

Table 1. Cont.

Solvent	λ_{\max} (nm) [lg ϵ (L mol ⁻¹ cm ⁻¹)]		
	Soret B (0,0)	Q (1,0)	Q (0,0)
<i>5-(3-hydroxyphenyl)-10,15,20-tris-phenyl-21,23-Zn(II)-porphine</i>			
PEG300	426 [5.820]	558 [4.358]	598 [4.000]
TX/water	426 [5.817]	559 [4.471]	599 [4.342]
TX/Chx	427 [5.991]	558 [4.408]	598 [4.017]
<i>5-(4-hydroxyphenyl)-10,15,20-tris-phenyl-21,23-Zn(II)-porphine</i>			
MeOH	422 [5.718]	557 [4.246]	596 [3.924]
DMSO	429 [5.702]	561 [4.246]	602 [4.017]
Chx	425 [5.729]	558 [4.292]	598 [3.903]
PEG300	427 [5.713]	559 [4.350]	599 [4.121]
TX/water	428 [5.709]	560 [4.255]	601 [3.982]
TX/Chx	427 [5.713]	560 [4.265]	600 [3.964]
<i>5-[(3,4-methylenedioxy)phenyl]-10,15,20-tris-(4-carboxymethylphenyl)-21,23-Zn(II)-porphine</i>			
MeOH	424 [5.686]	557 [4.255]	598 [3.880]
DMSO	431 [5.632]	562 [4.246]	603 [3.964]
Chx	425 [5.554]	558 [4.218]	599 [3.941]
PEG300	427 [5.577]	559 [4.221]	599 [3.940]
TX/water	428 [5.584]	559 [4.224]	602 [3.962]
TX/Chx	427 [5.579]	559 [4.226]	602 [3.963]
<i>5-(4-hydroxyphenyl)-10,15,20-tris-(4-carboxymethylphenyl)-21,23-Zn(II)-porphine</i>			
MeOH ¹	425 [5.732]	558 [4.342]	599 [4.049]
DMSO ¹	431 [5.800]	563 [4.246]	604 [4.028]
Chx	427 [5.571]	561 [4.255]	601 [3.826]
PEG300	426 [5.640]	558 [4.272]	599 [3.956]
TX/water	427 [5.570]	559 [4.232]	600 [3.980]
TX/Chx	426 [5.616]	558 [4.265]	598 [3.856]

MeOH = methanol; DMSO = dimethylsulfoxide; Chx = cyclohexane; PEG300 = polyethyleneglycol 300; TX = Triton X-100; ¹ Data were taken from [22].

Table 2. Wavelengths maxima (λ_{\max}) and molar extinction coefficient values (lg ϵ) for the copper porphyrinic complexes in different solvents and micellar media ($c = 2.5 \times 10^{-6}$ M).

Solvent	λ_{\max} (nm) [lg ϵ (L mol ⁻¹ cm ⁻¹)]	
	Soret B (0,0)	Q (1,0)
<i>5-(2-hydroxyphenyl)-10,15,20-tris-phenyl-21,23-Cu(II)-porphine</i>		
MeOH	411 [5.820]	537 [4.447]
DMSO	417 [5.769]	540 [4.505]
Chx	413 [5.843]	538 [4.447]
PEG300	416 [5.763]	539 [4.380]
TX/water	415 [5.838]	538 [4.505]
TX/Chx	416 [5.867]	539 [4.447]

Table 2. Cont.

Solvent	λ_{\max} (nm) [$\lg \epsilon$ (L mol ⁻¹ cm ⁻¹)]	
	Soret B (0,0)	Q (1,0)
5-(3-hydroxyphenyl)-10,15,20-tris-phenyl-21,23-Cu(II)-porphine		
MeOH	411 [5.780]	536 [4.422]
DMSO	418 [5.757]	542 [4.422]
Chx	414 [5.782]	538 [4.350]
PEG300	416 [5.763]	538 [4.350]
TX/water	416 [5.784]	539 [4.441]
TX/Chx	415 [5.766]	538 [4.415]
5-(4-hydroxyphenyl)-10,15,20- tris-phenyl - 21,23-Cu(II)-porphine		
MeOH	412 [5.701]	538 [4.422]
DMSO	420 [5.695]	542 [4.428]
Chx	414 [5.678]	539 [4.394]
PEG300	417 [5.684]	540 [4.326]
TX/water	416 [5.691]	539 [4.441]
TX/Chx	417 [5.701]	539 [4.537]
5-[(3,4-methylenedioxy)phenyl]-10,15,20-tris-(4-carboxymethylphenyl)-21,23-Cu(II)-porphine		
MeOH	414 [5.741]	538 [4.394]
DMSO	422 [5.652]	544 [4.408]
Chx	416 [5.770]	540 [4.371]
PEG300	417 [5.782]	540 [4.803]
TX/water	418 [5.792]	539 [4.800]
TX/Chx	418 [5.788]	540 [4.807]
5-(4-hydroxyphenyl)-10,15,20-tris-(4-carboxymethylphenyl)-21,23-Cu(II)-porphine		
MeOH ¹	414 [5.532]	539 [4.260]
DMSO ¹	423 [5.507]	545 [4.203]
Chx	419 [5.661]	540 [4.283]
PEG300	416 [5.782]	539 [4.150]
TX/water	416 [5.507]	539 [4.440]
TX/Chx	416 [5.766]	539 [4.415]

MeOH = methanol; DMSO = dimethylsulfoxide; Chx = cyclohexane; PEG300 = polyethyleneglycol 300; TX = Triton X-100; ¹Data were taken from [22].

The main differences observed in the spectral band position are due to the type of metallic ion. That means that the influence of the central ion is higher in what concerns the displacement of the spectral bands position compared to that induced by the peripheral substituents of the porphyrinic macrocycle, which is of only 2–4 nm. Therefore, in the case of Cu(II) complexes, Soret bands are 10–12 nm hypsochromically shifted compared to the corresponding Zn(II) complex having the same ligand, in the same solvent. Similarly, the Q bands of the copper porphyrins show a blue shift of about 20 nm compared to the corresponding zinc porphyrins. Results confirm earlier results obtained with other metalloporphyrins [22–24,26].

These spectral differences are the result of stronger conjugation effects that occur between the metallic ion orbitals and the π electrons of the tetrapyrrolic ring, effects that cause an energy decrease

of the a_{1u} (π) and a_{2u} (π) orbitals relative to the e_g (π^*) orbitals, with increased energy available for copper porphyrins that generate the blue shift of the spectral bands compared to the zinc porphyrins [28].

From the experimental data we could observe that the influence of the non-symmetrical substituents *versus* spectral properties of the metalloporphyrins is insignificant. The hydrophilic groups placed in various positions of the porphyrinic structure did not significantly disturb the inner π electron ring of the macrocycle, which is responsible for the active electronic transitions in the above mentioned spectral range [29,30].

The change of the charge density and distribution on the periphery of the porphyrine macrocycle induced by the polar substituents supports the localization of the photosensitizer at the cellular level, without significant change of the spectral properties responsible to its photophysical activation.

The organic solvents were chosen for the study taking into account their relative polarity, as defined by Reichard [31]. Thus, cyclohexane, dimethylsulfoxide and methanol, having relative polarity indices of 0.0006, 0.444 and 0.762, respectively, have been chosen. Only for comparison purposes, the ethylene glycol (relative polarity index 0.790) was also chosen.

The spectral data obtained indicate that the position of the absorption bands is less influenced by environmental polarity. However, a few observations can be made. For the same compound, the longest wavelengths maxima can be found in dimethylsulfoxide (generally, about 5 nm bathochromically shifted as compared to the other solvents), followed by cyclohexane and methanol (with 1 to 3 nm separate from each other). The observation is valid for both Soret and Q bands.

In case of direct micelles compared to PEG 300 (considered as reference), the shifts are too small (1–2 nm) or missing (in most cases in copper porphyrinic complexes). Meanwhile, the comparison of the wavelengths of the maxima with those belonging to the same compound dissolved in methanol (the most polar solvent) show that there is a slight bathochromic shift in case of the direct micelles *vs.* MeOH, suggesting the presumptive localization for the entire group of porphyrins as individual probe in direct micelles, as expected, in the polyethyleneoxide chain, at the interface with the *tert*-octyl-phenylether bulk of the TX-100 molecule, and not at the water-oxyethylene chain interface.

Similar results were obtained in the case of reverse micelles, *i.e.*, the maxima of the Soret bands position are in the same region as the PEG 300 reference system, indicating the metalloporphyrins localization at the oxyethylene chains level. The results confirm those obtained earlier on similar mesoporphyrinic compounds [32].

2.2. Fluorescence Spectroscopy

The fluorescence measurements were performed on the studied complexes in the same solvents and micellar systems. Only the zinc porphyrinic compounds exhibit fluorescent properties strong enough to be taken into account.

In order to get a good comparison between the compounds, the excitation was set to 420 nm.

One can observe that the differences between the emission wavelengths are small, confirming the results already obtained for the absorption spectra. Therefore, the fluorescence spectral data shows for zinc porphyrinic complexes two bands located in the spectral region of 605–665 nm (Figure 4, Table 3) and reveal smaller shifts of the emission maxims when changing the environmental polarity. This small

bathochromic shift of the fluorescence maximum position indicates incorporation of the porphyrinic complex in the micellar media.

Figure 4. Fluorescence emission of 5-(4-hydroxyphenyl)-10,15,20-*tris*-phenyl-21,23-Zn(II)-porphine in different solvents and micellar solutions ($c = 2.5 \times 10^{-6}$ M, $\lambda_{\text{ex}} = 420$ nm).

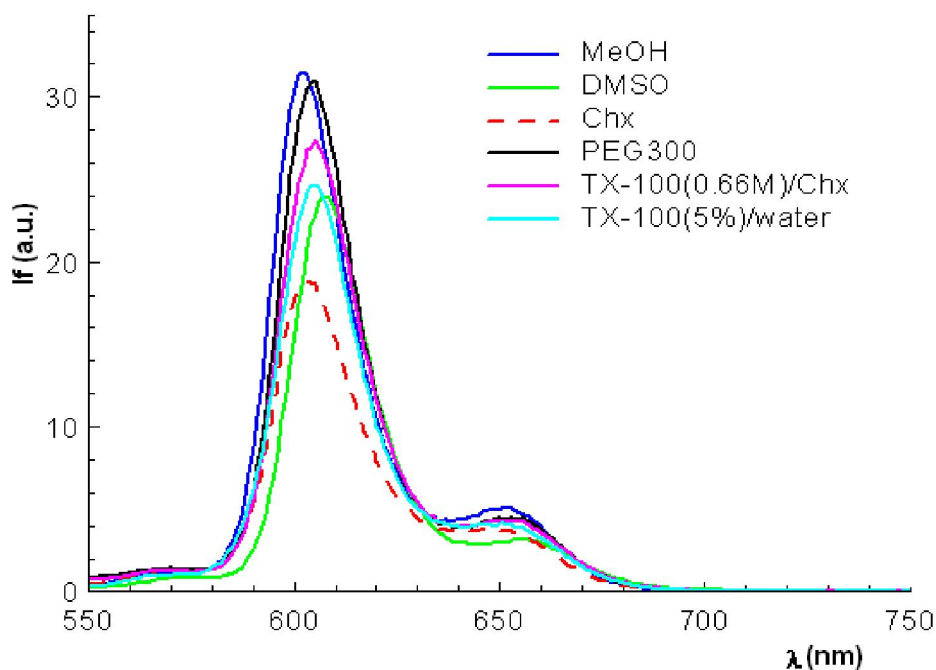


Table 3. Fluorescence emission peak wavelength of the zinc mesoporphyrinic complexes in solvents with different polarities and micellar media ($c = 2.5 \times 10^{-6}$ M, $\lambda_{\text{ex}} = 420$ nm).

Solvent	λ_{max} (nm)	
<i>5-(2-hydroxyphenyl)-10,15,20-tris-phenyl-21,23-Zn(II)-porphine</i>		
MeOH	600	651
DMSO	605	654
Chx	602	651
PEG300	602	651
TX/water	603	652
TX/Chx	602	651
<i>5-(3-hydroxyphenyl)-10,15,20-tris-phenyl-21,23-Zn(II)-porphine</i>		
MeOH	600	650
DMSO	605	656
Chx	605	656
PEG300	602	652
TX/water	603	652
TX/Chx	603	651
<i>5-(4-hydroxyphenyl)-10,15,20-tris-phenyl-21,23-Zn(II)-porphine</i>		
MeOH	602	651
DMSO	608	655

Table 3. Cont.

Solvent	λ_{\max} (nm)	
<i>5-(4-hydroxyphenyl)-10,15,20-tris-phenyl-21,23-Zn(II)-porphine</i>		
Chx	602	652
PEG300	605	653
TX/water	605	653
TX/Chx	605	651
<i>5-[(3,4-methylenedioxy)phenyl]-10,15,20-tris-(4-carboxymethylphenyl)-21,23-Zn(II)-porphine</i>		
MeOH	605	652
DMSO	610	658
Chx	604	650
PEG300	605	662
TX/water	606	665
TX/Chx	605	665
<i>5-(4-hydroxyphenyl)-10,15,20-tris-(4-carboxymethylphenyl)-21,23-Zn(II)-porphine</i>		
MeOH ¹	605	652
DMSO ¹	611	656
Chx	604	652
PEG300	605	663
TX/water	606	665
TX/Chx	606	665

MeOH = methanol, DMSO = dimethylsulfoxide, Chx = cyclohexane, PEG300 = polyethylene glycol 300, TX = Triton X-100; ¹ Data were taken from [22].

In Triton X-100/cyclohexane reverse micelles the fluorescence data of zinc complexes confirm their localization in the area of the polyethyleneoxidic chains, as the maximum wavelength is located in the same spectral range as in the PEG 300 reference system.

For the zinc tetrapyrrolic complexes a smaller bathochromic shift in direct micelles was registered as compared to PEG 300 systems and methanolic solution, suggesting a localization of the complex in the polar area of the micelle.

The results indicate that the administration of the porphyrins to cells in view of photosensitization will probably not change the photophysical characteristics of the porphyrins even embedded in liposomes or other kind of delivery systems.

The Stokes shifts of the studied Zn(II) mesoporphyrins, computed as the difference between the maximum of emission and that one of absorption, as displayed in Table 4, show that the influence DMSO compared to the other two solvents used results in less change of the Stokes shift (of 1 to 3 nm).

Table 4. Stokes shifts ($\lambda_{em} - \lambda_{abs}$) for the Zn(II) complexes [nm].

Porphyrinic complexes	$\lambda_{em} - \lambda_{abs}$ [nm]					
	MeOH	DMSO	Chx	PEG300	TX-100/w	TX-100/Chx
Zn(II)TPPOHo	179	177	177	177	176	175
Zn(II)TPPOHm	179	177	176	176	177	176
Zn(II)TPPOHp	180	179	177	178	177	178
Zn(II)TRMOPP	181	179	179	178	178	178
Zn(II)TCMPOHp	180	180	177	179	179	180

3. Experimental Section

Porphyritic complexes used in this study were synthesized as previously described [22–24].

Poly (oxyethylene) tert-octylphenyl ether (Triton X-100–TX, purity > 99%), methanol (MeOH, HPLC gradient grade), dimethyl sulfoxide (DMSO, analytical grade) dichloromethane (analytical grade) and polyethylene glycol 300 (Carbowax 300) were bought from Sigma and used without supplementary preparation before. Water was double distilled and deionized before use.

Molecular absorption spectra were recorded on a Lambda 35 Perkin-Elmer UV-Vis spectrophotometer in 10 mm path length quartz cells, in single beam mode.

Fluorescence spectra were recorded on a steady-state Jasco FP 6500 spectrofluorimeter in 10 mm path length quartz cells.

The solutions used were prepared by repeated dilution to obtain a final 2.5×10^{-6} M concentration of each compound in the three solvents.

The 0.24 mM TX-100 in water (w/w) direct micelles (DM) and 0.66 M TX-100 in cyclohexane (w/w) reverse micelles (RM) loaded with 2.5×10^{-6} M metalloporphyrins were prepared according to the procedure described before [33]. Briefly, appropriate volumes of metalloporphyrins in dichloromethane solutions were evaporated to dryness at room temperature on the bottom of a test tube. Aliquots of 3mL of appropriate concentrations of Triton X-100 in water and cyclohexane were added, and then the tubes were mildly vortex mixed for 5 minutes, capped and then left still overnight to ensure the solubilization and diffusion of the metalloporphyrins into the micelles. The final concentration of each porphyritic compound in micellar media was set at 2.5×10^{-6} M; the solutions were kept in dark to prevent photodegradation before the measurements, which were performed 24 h after preparation.

4. Conclusions

The paper presents the molecular spectral characteristics of certain A_3B type *meso*-substituted metalloporphyrins in different polarity solvents and in micellar media. The studies revealed that the position of Soret and Q bands of the porphyrins is mainly influenced by the central metal ion and less by the peripheral substituents of the porphyritic core or polarity of the solvent, thus confirming the results previously obtained on other metalloporphyrins.

The estimated localization of the porphyritic in direct and reversed micelles compounds was possible by the evaluation of the spectral changes, for each compound, using PEG 300 as reference *versus* TX-100 (0, 66 M)/cyclohexane and TX-100 (5% g/g)/water, accounting simultaneously for the micropolarity of the oxyethylenic chains and of the hydrophilic and hydrophobic parts of micellar systems. For all compounds, the localization at the interface between the polyethylene oxide chains and the *tert*-octyl-phenyl etheric residue of the Triton X-100 molecules was considered most probable. The steady-state fluorescence emission studies confirm the results obtained by UV-Vis absorption in what concerns the small differences between the maximum emission peak in correlation to the chemical structure of the porphyrin and in the lack of correlation between the position of the bands and the solvent polarity as defined by Reichard. All these findings suggest that the photophysical properties of the compounds will not be dramatically changed if the compounds are embedded in liposomes to obtain a better delivery to the cellular target.

Acknowledgments

This research was supported by CNMP project No. 41–047/2007 and ERA NET project No. 7–030/2010 the Romanian Ministry of Education and Research

References

1. Santiago, P.S.; Netoa, D.S.; Gandini, S.C.M.; Tabak, M. On the localization of water-soluble porphyrins in micellar systems evaluated by static and time-resolved frequency-domain fluorescence techniques. *Colloid. Surface B* **2008**, *65*, 247–256.
2. Gandini, S.C.M.; Yushmanov, V.E.; Tabak, M. Interaction of Fe(III)- and Zn(II)-tetra(4-sulfonatophenyl) porphyrins with ionic and nonionic surfactants: Aggregation and binding. *J. Inorg. Biochem.* **2001**, *85*, 263–277.
3. Scolaro, L.M.; Donato, C.; Castriciano, M.; Romeo, A.; Romeo, R. Micellar aggregates of platinum(II) complexes containing porphyrins. *Inorg. Chim. Acta* **2000**, *300*, 978–986.
4. Berg, K.; Selbo, P.K.; Weyergang, A.; Dietze, A.; Prasmickaite, L.; Bonsted, A. Porphyrin related photosensitizers for cancer imaging and therapeutic. *J. Microsc.* **2005**, *218*, 133–147.
5. Chatterjee, D.K.; Yong, Z. Nanoparticles in photodynamic therapy: An emerging paradigm. *Adv. Drug Deliv. Rev.* **2008**, *60*, 1627–1637.
6. Bonneau, S.; Bizet, C.V.; Mojzisova, H.; Brault, D. Tetrapyrrole-photosensitizers vectorization and plasma LDL: A physic-chemical approach. *Int. J. Pharm.* **2007**, *344*, 78–87.
7. Boyle, R.W.; Dolphin D. Structure and biodistribution relationships of photodynamic sensitizers. *Photochem. Photobiol.* **1996**, *64*, 469–485.
8. Weitemeyer, A.; Kliesch, H.; Michelsen, U.; Hirth, A.; Wöhrle, D. Unsymmetrically Substituted Porphyrazines. In *Photodynamic Tumor Therapy: Second and Third Generation Photosensitizers*; Moser, J.G., Ed.; Harwood: New Delhi, India, 1998; pp. 87–99.
9. Sandberg, S.; Romslo, I. Porphyrin-induced photodamage at the cellular and the subcellular level as related to the solubility of the porphyrin. *Clin. Chim. Acta* **1981**, *109*, 193–201.
10. Ricchelli, F. Photophysical properties of porphyrins in biological membranes. *J. Photochem. Photobiol. B* **1995**, *29*, 109–118.
11. Gandini, S.C.M.; Yushmanov, V.E.; Borissevitch, I.E.; Tabak, M. Interaction of the tetra (4-sulfonatophenyl)porphyrin with ionic surfactants: Aggregation and location in micelles. *Langmuir* **1999**, *15*, 6233–6243.
12. Correa, N.M.; Durantini, E.N.; Silber, J.J. substituent effects on binding constants of carotenoids to *n*-heptane/AOT reverse micelles. *J. Colloid Interface Sci.* **2001**, *240*, 573–580.
13. Suchetti, C.A.; Durantini, E.N. Monomerization and photodynamic activity of Zn(II) tetraalkyltetrapyridinoporphyrazinium derivatives in AOT reverse micelles. *Dye. Pigment.* **2007**, *74*, 630–635.
14. Correa, N.M.; Durantini, E.N.; Silber, J.J. Binding of nitrodiphenylamines to reverse micelles of AOT in *n*-hexane and carbon tetrachloride: Solvent and substituent effects. *J. Colloid Interface Sci.* **1998**, *208*, 96–103.

15. Battah, S.; O'Neill, S.; Edwards, C.; Balaratnam, S.; Dobbin, P.; MacRobert, A.J. Enhanced porphyrin accumulation using dendritic derivatives of 5-aminolaevulinic acid for photodynamic therapy: An *in vitro* study. *Int. J. Biochem. Cell Biol.* **2006**, *38*, 1382–1392.
16. Medhage, B.; Almgren, M. Diffusion-influenced fluorescence quenching dynamics in one to three dimensions. *J. Fluoresc.* **1992**, *2*, 7–21.
17. Barghouthi, S.A.; Perrault, J.; Holmes, L.H. Effect of solvents on the fluorescence emission spectra of 1-anilino-8-naphthalene sulfonic acid: A physical chemistry experiment. *Chem. Educ.* **1998**, *3*, 1–5.
18. Shen, D.; Zhang, R.; Han, B.; Dong, Y.; Wu, W.; Zhang, J.; Li, J.; Jiang, T.; Liu, Z. Enhancement of the solubilization capacity of water in triton X-100/cyclohexane/water system by compressed gases. *Chemistry* **2004**, *10*, 5123–5128.
19. Medhage, B.; Almgren, M.; Alsins, J. Phase structure of poly(oxyethylene) surfactants in water studied by fluorescence quenching. *J. Phys. Chem.* **1993**, *97*, 7753–7762.
20. Zhu, D.M.; Wu, X.; Schelly, Z.A. Reverse micelles and water in oil microemulsions of Triton X 100 in mixed solvents of benzene and n-hexane. Dynamic light scattering and turbidity studies. *Langmuir* **1992**, *8*, 1538–1540.
21. Harris, J.M.; Chess, R.B. Effect of pegylation on pharmaceuticals. *Nat. Rev. Drug Discov.* **2003**, *2*, 214–221.
22. Boscencu, R. Asymmetrical mesoporphyrinic complexes of Copper (II) and Zinc (II). Microwave-assisted synthesis, spectral and cytotoxicity evaluation. *Molecules* **2011**, *16*, 5604–5617.
23. Boscencu, R.; Socoteanu, R.; Oliveira, A.S.; Vieira Ferreira, L.F.; Nacea, V.; Patrinoiu, G. Synthesis and characterization of some unsymmetrically-substituted mesoporphyrinic monohydroxyphenyl complexes of Copper(II). *Pol. J. Chem.* **2008**, *82*, 509–522.
24. Boscencu, R.; Socoteanu, R.; Oliveira, A.S.; Ferreira, L.F.V. Studies on Zn(II) monohydroxyphenyl mesoporphyrinic complexes. Synthesis and characterization. *J. Serb. Chem. Soc.* **2008**, *73*, 713–726.
25. Mack, J.; Stilman, M.J. Electronic Structure of Metal Phtalocyanine and Porphyrin Complexes from Analysys of UV-Visible Absorption and Magnetic Circular Dichroism Spectra and Molecular Orbital Calculations. In *The Porphyrin Handbook*; Kadish, K.M., Smith, K.M., Guillard, R., Eds.; Academic Press: San Diego, CA, USA, 2003; Volume 16, pp. 43–52.
26. Gouterman, M. Optical Spectra and Electronic Structure of Porphyrins and Related Rings. In *The Porphyrins*; Dolphin, D., Ed.; Academic Press: New York, NY, USA, 1978; Volume III, pp. 1–165.
27. Boscencu, R.; Ilie, M.; Socoteanu, R.; Oliveira, A.S.; Constantin, C.; Neagu, M.; Manda, G.; Vieira Ferreira, L.F. Microwave synthesis, basic spectral and biological evaluation of some Copper (II) mesoporphyrinic complexes. *Molecules* **2010**, *15*, 3731–3743.
28. Gouterman, M.; Wagniere, G.H.; Snyder, L.C. Spectra of porphyrins: Part II. Four orbital model. *J. Mol. Spectrosc.* **1963**, *11*, 108–127.
29. Harriman, A. Luminescence of porphyrins and metalloporphyrins. *J. Chem. Soc. Faraday Trans.* **1981**, *77*, 369–377.
30. Quimby, D.J.; Longo, F.R. Luminescence studies on several tetraarylporphins and their Zinc derivatives. *J. Am. Chem. Soc.* **1975**, *97*, 5111–5117.

31. Reichard, C.; Welton, T. *Solvents and Solvent Effects in Organic Chemistry*, 4th ed.; Wiley-VCH: Hoboken, NJ, USA, 2010.
32. Boscencu, R.; Socoteanu, R.; Ilie, M.; Bandula, R.; Sousa, O.A.; Vieira Ferreira, L.F. Spectral properties of Copper (II) and Zinc(II) complexes with mesoporphyrinic ligands in micellar media. *Rev. Chim.* **2010**, *61*, 135–139.
33. Carageorgheopol, A.; Bandula, R.; Caldararu, H.; Joela, H. Polarity profiles in reverse micelles of Triton X-100, as studied by spin probe and absorption probe techniques. *J. Mol. Liq.* **1997**, *72*, 105–119.

© 2011 by the authors; licensee MDPI, Basel, Switzerland. This article is an open access article distributed under the terms and conditions of the Creative Commons Attribution license (<http://creativecommons.org/licenses/by/3.0/>).